HCl (10 mM). Diethyl ether solution containing MPAz was dehydrated using anhydrous magnesium sulfate. After filtration to remove magnesium sulfate, the solvent was evaporated under reduced pressure, yielding MPAz in the form of a light yellow oily liquid. Upon freezing, MPAz was converted into a solid. The chemical structure of MPAz was confirmed using ^{1}H NMR in $CDCl_3$ and Fourier-transform infrared spectroscopy (FT-IR) (FT-IR-615, Jasco, Tokyo, Japan). NMR (ppm): 1.95 (d, 3H, α-CH_3), 4.56 (d, 4H, $-CH_2CH_2$), 5.59 (d, 1H, $=CH_2$), 6.14 (d, 1H, $=CH_2$), 7.07 (d, 2H, benzyl), 8.06 (d, 2H, benzyl). IR(cm^{-1}): 3021(p-Ar), 2124 (C–N_3), 1720 (C=O), 1604 (C=C).

Poly(MPC-*co*-MPAz) (PMAz) was synthesized by a conventional radical polymerization method in ethanol using AIBN as a radical polymerization initiator. The desired amounts of MPC and MPAz (monomer molar fractions were 0.70 and 0.30, respectively, and total monomer concentration was 0.50 M) and AIBN (2.5 mM) were used for polymerization. Polymerization was carried out at 60 °C for 3.5 h. The reaction mixture was poured in an excess volume of diethyl ether/chloroform (80/20 v/v) to precipitate the polymer. The precipitated polymer was collected and purified by dialysis against water using a dialysis membrane (cutoff molecular weight=3000). Next, the polymer was freeze-dried. The chemical structure of the PMPAz was confirmed using ^{1}H NMR in CD_3CD_2OD. Molecular weight of the polymers was evaluated using GPC in a mixture of water and methanol (30:70 v/v), and its retention time was compared with that of the poly(ethylene glycol) standard (Tosoh Co., Tokyo, Japan). The chemical structure of PMPAz is shown in Fig. 1.

2.4. Quartz substrate preparation

Alkyl groups were introduced on the quartz substrate to react with PMAz. After cleaning using oxygen plasma (PR500 plasma reactor; Yamato Science, Tokyo, Japan) (300 W, 100 mL/min flow) for 10 min, quartz substrates were placed in toluene solution containing *n*-butyltrichlorosilane (50 mmol) and 2-(carbomethoxy)-ethyltrichlorosilane (50 mmol) for 1 h at room temperature. Next, the quartz substrate was washed by sonication using toluene and methanol.

2.5. Protein stamp preparation

PMSiN was reacted with the surface of silica beads to immobilize imprinted proteins. The 0.50 g of beads were cleaned using oxygen plasma and placed in a 50-mL Eppendorf tube. Subsequently, 25 mL of ethanol solution containing 0.20 wt% PMSiN was added to the tube containing silica beads, and the tube was rotated for 1 h at room temperature. Beads were filtered and transferred to a Teflon® dish for solvent evaporation under atmospheric pressure. Next, the beads were heated at 70 °C for 3 h to react PMSiN with the silica beads. The beads were transferred to a 50-mL Eppendorf tube and washed with ethanol for 1 h to remove unreacted PMSiN, after which they were filtered and dried under a vacuum.

PMSiN–silica beads (10 mg) were placed into Eppendorf tubes. BSA or OVA solution (1.0 mg/mL, pH 7.8 phosphate buffer solution) was added to the each tube. Tubes were rotated at 4 °C for 48 h to immobilize the protein, and the amount of immobilized BSA and OVA on PMSiN–silica beads was determined on the basis of the UV absorbance of the supernatant at 400 nm by using UV/visible spectroscopy (V-560, Jasco Co., Tokyo, Japan); absorbance was based on the *p*-nitrophenoxy anion released during the protein immobilization reaction. After rinsing the beads with pH 7.8 phosphate buffer solution for 10 min, the remaining active ester groups were deactivated using a glycine-containing solution (1.0 mg/mL, pH 7.8 PBS) at 4 °C for 24 h. Beads immobilized with BSA and OVA were rinsed with water for 10 min and the water was removed. This procedure was repeated 3 times. Protein-immobilized beads were used as protein stamp beads.

2.6. Protein imprinting surface preparation

Protein stamp beads were mixed with an aqueous solution containing PMPAz and SDS. The silica bead suspension was placed on the quartz substrate with modified alkyl groups and was dried at 25 °C. Substrates were irradiated using a UV lamp (UV Cross-linker, CL-1000, 254 nm, Funakoshi, Tokyo, Japan) for 1 min (light intensity=80 J/cm^2). Following the photoreaction, protein stamp beads were detached from the substrate via sonication for 10 s. A non-molecular imprinting surface (NMIP) was also prepared using silica beads that had not been subjected to protein immobilization. The morphology of the MIP substrate was observed using a scanning electron microscope (SEM; SM-200, Topcon, Tokyo, Japan). We fabricated MIP on the polyethylene substrate by using same procedure and measured the thickness of the PMPAz layer using an atomic force microscopic (AFM; Nanoscope IIIa, Nihon Veeco, Tokyo, Japan). The thickness was in the range between 100 nm and 400 nm. Furthermore, the BSA structure during MIP process was confirmed using a circular dichroism measurement (CD; J-720W, Jasco, Tokyo, Japan). Before and after photoreaction, the molar ellipticity was $-16{,}576.5°$ cm^2 $dmol^{-1}$ and $-16{,}340.8°$ cm^2 $dmol^{-1}$ at 222 nm, and α-helix content was 41.4% and 40.9%, respectively. In the SDS containing solution (molar ratio of BSA and SDS is 1:5), the molar ellipticity was $-16{,}261.5°$ cm^2 $dmol^{-1}$ at 222 nm, and the α-helix content was 40.1%. The CD spectrum was not changed during photoreaction and in the SDS solutions. The BSA did not have any adverse effect during photoreaction.

2.7. Target protein detection

Capture of target proteins was detected using UVFLIM. UVFLIM consists of a 266-nm UV mode-locked diode-pumped picosecond laser (model GE-100-XHP-FHG, Time-Bandwidth Products, Inc., Switzerland). The laser system provides pulses with a duration of <10 ps and a repetition rate of 40 MHz; the laser has a maximum power output of 30 mW. The laser power was adjusted by inserting different neutral density filters (Melles Griot). The polarized laser beam was split 50/50 by a beam splitter (Laser Components GmbH, Germany), sending 50% into a high-speed photodiode module (Becker & Hickl GmbH, Berlin, Germany), which is used as deriving the synchronization signal for triggering of the time-correlated single-photon (TCSPC) module. The second beam passed an excitation filter (model 254WB25, Omega Optical) and is directed into the quartz microscope objective (40×, NA=0.80, Partec GmbH, Münster, Germany) by a dichroic beam splitter (model 290DCLP, Omega Optical). Surface scans were performed by moving the sample with a motorized *x*,*y*-translation stage (Märzhäuser, Wetzlar, Germany). The fluorescence light was collected by the same objective and transmitted through the dichroic mirror. An achromatic lens (LAU-25-200, OFR Inc., 200 mm focal distance) focuses the light onto a pinhole. After the pinhole, the fluorescence emission is detected by a high-speed photomultiplier tube (PMT) detector head (model PMH-100-6, Becker & Hickl GmbH). Two emission band-pass filters (model 330WB60, Omega Optical) -one positioned directly after the lens, and the other positioned directly in front of the detector-discriminate fluorescence against scattered light. The signal pulse of the PMT were fed into a TCSPC PC interface card (SPC-630, Becker & Hickl GmgH, Berlin, Germany) to acquire fluorescence signal. A software using C++ program was developed for synchronization of the scanning motion with the

data acquisition and recording the fluorescence intensity imaging. After adding BSA solution (2×10^{-6} M) and OVA solution (2×10^{-6} M) to the NMIP, the BSA-MIP and the OVA-MIP substrates for 2 h, substrates were rinsed with water and dried under N_2 gas. The substrates were placed onto the *x*,*y* scanning stage and intrinsic tryptophan emission was recorded after one-photon excitation at 266 nm. The microscopy objective of UVFLIM focuses laser beam to a size of the illumination point about 1 μm in diameter and 3 μm deep. When we take scanning images, we are able to measure all fluorescence generated from MIP protein layer (thickness between 100 nm and 400 nm). The fluorescence intensity of all samples was normalized to same intensity level using MATLAB software.

3. Results and discussion

3.1. Characterization of protein stamps

Silica beads (diameter: 15 μm) were used as MIP stamp substrates for protein imprinting. We designed PMSiN to immobilize the imprinted protein on the surface of silica beads (Fig. 1). PMSiN can react with the MPTS unit on the silica bead surface via a silane coupling reaction, and imprinted proteins can be immobilized using the MEONP unit. MPC units play an important role in immobilized protein stabilization. After the reaction, successful construction of the PMSiN layer was confirmed using XPS analysis. High signal intensities were observed at 402 eV in the N_{1s} region and at 133 eV in the P_{2p} region, which was attributed to the MPC unit. The total amount of MEONP units on the silica beads (6.6×10^{-10} mol/mg) was evaluated using UV spectroscopy after complete hydrolysis of the *p*-nitrophenyloxycarbonyl units in 0.20 M NaOH aqueous solution. The active ester group is labile to the primary amino group of the biomolecules, and a carbamate linkage is produced after bioconjugation (Watanabe and Ishihara, 2006). The amounts of immobilized BSA and OVA were 3.3×10^{-10} mol and 3.2×10^{-10} mol, respectively. Approximately 50% of the active ester group was used to immobilize the proteins, and the remaining active groups were deactivated through reaction with glycine. Protein-immobilized silica beads were used as protein stamps for preparing the MIP surface.

3.2. Characterization of protein MIP substrate

The process for preparing the protein MIP substrate is summarized in Fig. 2. The conformation of proteins is flexible and fragile. Therefore, the ligand should be arranged in a suitable position against the imprinted protein to construct the protein recognition site. It is well known that the surfactant can bind to protein via hydrophobic and electrostatic interactions (Mackie and Wilde, 2005; Sonesson et al., 2008). We employed SDS, an anionic surfactant, as a ligand for specific binding of BSA and OVA. At the lowest concentration of 0.10 mM SDS, 6 SDS molecules were bound per BSA without causing denaturation (Turro et al., 1995; Vasilescu and Angelescu, 1999). In this study, an SDS molecule number that was 5 times larger than the molecules of the immobilized imprinted protein was applied. As a control, the MIP process was carried out without SDS. Other important aspect of protein MIP is suppressing non-specific protein adsorption to the region outside the recognition site. We designed a photoreactive water-soluble polymer, PMPAz (Fig. 1), to prepare the matrix. PMPAz possesses both phosphorylcholine groups and azido groups. Polymers with phosphorylcholine groups effectively suppress nonspecific protein adsorption and cell adhesion due to the nature of the phosphorylcholine groups (Marra et al., 1997; Lu et al., 2001; Inoue and Ishihara, 2010). Azide groups decompose due to UV irradiation, forming nitrene groups, which generate highly reactive radicals. These radicals can attack alkyl groups, which were introduced to the surface and SDS. Thus, the matrix, which exhibits resistance to protein adsorption, was prepared after photoreaction. Ligands bound to the target protein were fixed using PMPAz. After the photoreaction, protein stamps were physically removed from the aqueous medium. The morphology of the quartz substrate was observed using SEM (Fig. 3). Silica beads produced 7-μm dimple-shaped patterns. This indicates that PMPAz reacted with alkyl groups on the quartz substrate to form a thick layer that embedded some of the silica beads.

3.3. Selective capturing of target proteins

It is important to remove imprinted molecules from the matrix after polymerization because target protein capture depends on this removal. The fluorescence based on tryptophan (Trp) residue

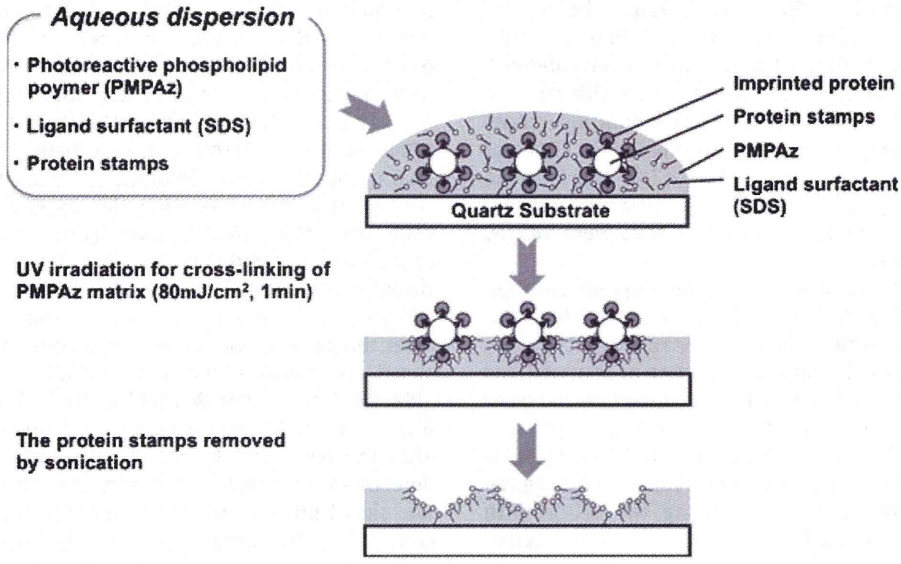

Fig. 2. Procedure for imprinting substrate using molecular integration.

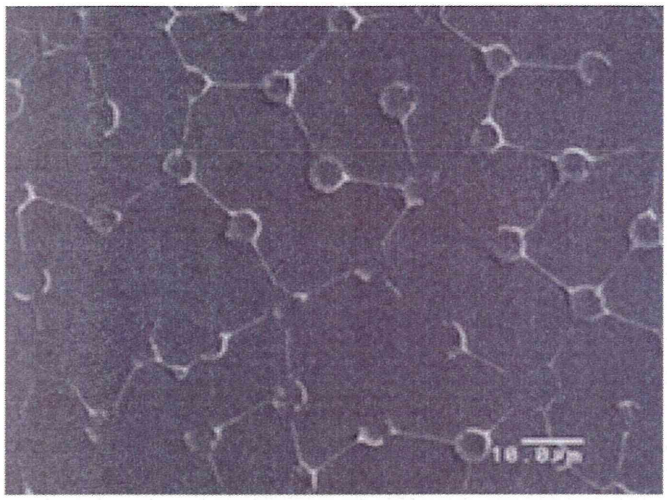

Fig. 3. SEM observation of substrate removing silica beads after photoreaction of PMPAz.

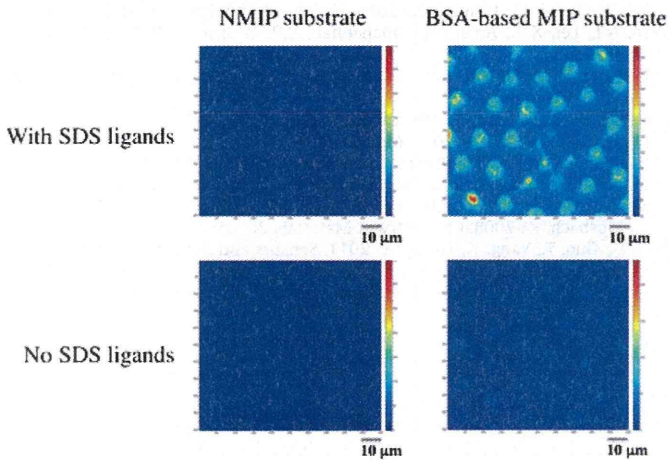

Fig. 4. Fluorescence intensity images by UVFILM after contact with BSA solution to NMIP and BSA-based MIP.

of protein was observed by UVFLIM. Before target protein addition, substrate fluorescence was not observed, indicating that the imprinted protein had been completely removed from the matrix after photoreaction. Fluorescence intensity after addition of the BSA solution to NMIP and BSA-based MIP with or without ligand is shown in Fig. 4. No fluorescence was observed for the NMIP substrates with or without the SDS ligand. Thus, BSA was not captured on these substrates. Additionally, non-specific protein adsorption was suppressed on the PMPAz surface. We observed a strong, dimple-shaped fluorescence pattern on the BSA based-MIP substrate with SDS ligand, and no fluorescence was observed on the BSA based-MIP substrate without ligand. SEM images shown in Fig. 3 were compared with dimple-shaped fluorescent regions, corresponding to the region of protein stamp contact. The target protein, BSA, was captured on the region where BSA was imprinted. We prepared molecular recognition sites on the non-specific protein adsorption surface using this MIP process. The arrangement of SDS ligands against the imprinted protein is important for capturing target proteins because fluorescence was not observed on the substrate.

Both BSA-based MIP and OVA-based MIP substrates were prepared to confirm selective capturing. UVFILM results are shown in Fig. 5. Molecular parameters of BSA and OVA are summarized in Table 1. These molecules possess a different number of aromatic

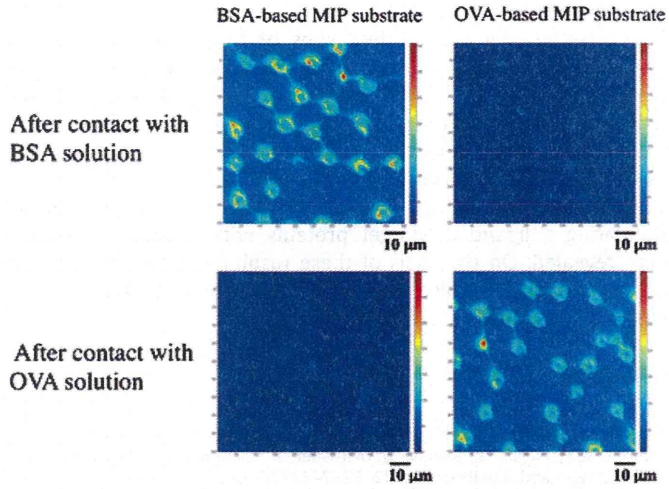

Fig. 5. Fluorescence intensity images by UVFILM after contact with BSA or OVA solution to the BSA-based MIP substrate and OVA-based MIP substrate.

Table 1
Chemical parameters of BSA and OVA.

Protein	Mw (kDa)	pI	Number of amino acid residue in molecule	Aromatic amino acid residues		
				Trp	Tyr	Phe
BSA	69.3	5.82	607	3	21	30
OVA	42.9	5.19	386	3	10	20

amino acid residues, including Trp, tyrosine (Tyr), and phenylalanine (Phe), which contribute to intrinsic fluorescence. However, the intrinsic fluorescence of Tyr is approximately 100 times weaker than that of Trp due to a low extinction coefficient, while the fluorescence emission of Phe is negligible due to a low extinction coefficient and low quantum efficiency. Additionally, transmission of Tyr and Phe fluorescence through our emission filter set is very low due to the blue-shifted emission maximum relative to Trp. Therefore, the intrinsic fluorescence of BSA and OVA was dominated by Trp residues. We can consider fluorescent intensity to represent the degree of adsorption because both BSA and OVA have the same number of Trp residues in 1 molecule. After contact with BSA in BSA-based MIP and OVA-based MIP, we observed strong fluorescence only on the BSA-based MIP substrate. In contrast, after contact with OVA, we observed strong fluorescence only on the OVA-based MIP substrate. Selective capturing against target proteins was observed for the protein MIP substrate. Equal numbers of SDS molecules as a ligand was used, and BSA and OVA have nearly the same isoelectric point. These results indicate that protein capture was not derived from a simple electrostatic interaction between proteins and SDS ligands. A suitable arrangement and density of SDS ligands is important for selective capturing on a substrate. UVFILM does not require molecular labeling of the protein and is sufficiently sensitive to detect low protein levels. Molecular labeling is perhaps disturbed the capturing the target proteins due to change in the chemical and structural nature of the proteins. Here, we showed that UVFILM is a powerful tool for detecting protein capturing on an MIP substrate.

4. Conclusion

Protein recognition sites were artificially constructed on a quartz substrate using the MIP process. Target protein capture

was detected by label-free detection using deep-UVFILM. We demonstrated that the binding sites of target proteins, BSA or OVA, were successfully constructed by integration of SDS molecules by applying 2 types of MPC polymers. MPC polymers provided resistance to non-specific protein adsorption and specificity to the MIP portions. The MIP surface exhibited good selectivity between BSA and OVA based on corresponding MIP proteins, despite having similar isoelectric points. The importance and effectiveness of integrating a ligand for target proteins with a suitable position were revealed. On the basis of these results, we suggest that our new protein MIP surface used in combination with UVFLIM is a versatile system for sensing biomolecules.

References

Ansell, R.J., Mosbach, K., 1997. Journal of Chromatography A 787, 55–66.
Belmont, A.S., Jaeger, S., Knopp, D., Niessner, R., Gauglitz, G., Haupt, K., 2007. Biosensors and Bioelectronics 22, 3267–3272.
Berney, H., Roseingrave, P., Aldermen, J., Lane, W., Collins, J.K., 1997. Sensors and Actuators B 44, 341–349.
Fu, G., Zhao, J., Yu, H., Liu, Li., He, B., 2007. Reactive and Functional Polymers 67, 442–450.
Fukazawa, K., Ishihara, K., 2009. Biosensors and Bioelectronics 25, 609–614.
Goto, Y., Matsuno, R., Konno, T., Takai, M., Ishihara, K., 2008. Macromolecules 9, 828–833.
Hall, W.P., Ngatia, S.N., Van Duyne, R.P., 2011. Journal of Physical Chemistry C 115, 1410–1414.
Hua, Z., Chen, Z., Li, Y., Zhao, M., 2008. Langmuir 24, 5773–5780.
Ibii, T., Kaieda, M., Hatakeyama, S., Shiotsuka, H., Watanabe, H., Umetsu, M., Kumagai, I., Imamura, T., 2010. Analytical Chemistry 82, 4229–4235.
Inoue, Y., Ishihara, K., 2010. Colloids and Surfaces B: Biointerfaces 81, 350–357.
Ishihara, K., Ueda, T., Nakabayashi, N., 1990. Polymer Journal 22, 355–360.
Ishihara, K., Ziats, N.P., Tierney, B.P., Nakabayashi, N., Anderson, James M., 1991. Journal of Biomedical Materials Research 25, 1397–1407.
Ishihara, K., Nomura, H., Mihara, T., Kurita, K., Iwasaki, Y., Nakabayashi, N., 1998. Journal of biomedical materials research 39, 323–330.
Konno, T., Watanabe, J., Ishihara, K., 2004. Biomacromolecules 5, 342–347.
Kryscio, D.R., Peppas, N.A., 2012. Acta Biomaterialia 8, 461–473.
Li, Q., Ruckstuhl, T., Seeger, S., 2004. Journal of Physical Chemistry B 108, 8324–8329.
Li, Q., Seeger, S., 2006. Analytical Chemistry 78, 2732–2737.
Li, Q., Seeger, S., 2009. Sensors and Actuators B 139, 118–124.
Li, Q., Seeger, S., 2011. Journal of Physical Chemistry B 115, 13643–13649.
Lu, J.R., Murphy, E.F., Su, T.J., Lewis, A.L., Stratford, P.W., Satija, S.K., 2001. Langmuir 17, 3382–3389.
Mackie, A., Wilde, P., 2005. Advances in Colloid and Interface Science 117, 3–13.
Marra, K.G., Winger, T.M., Hanson, S.R., Chaikof, E.L., 1997. Macromolecules 30, 6483–6488.
Mieda, S., Amemiya, Y., Kihara, T., Okada, T., Sato, T., Fukazawa, K., Ishihara, K., Nakamura, N., Miyake, J., Nakamura, C., 2012. Biosensors and bioelectronics 31, 323–329.
Murphy, E.P., Lu, J.R., Brewer, J., Russell, J., Penfold, J., 1999. Langmuir 15, 1313–1322.
Nishizawa, N., Konno, T., Takai, M., Ishihara, K., 2008. Macromolecules 9, 403–407.
Osawa, T., Shirasaka, K., Matsui, T., Yoshihara, S., Akiyama, T., Hishiya, T., Asanuma, H., Komiyama, M., 2006. Macromolecules 39, 2460–2466.
Sakaki, S., Nakabayashi, N., Ishihara, K., 1999. Journal of Biomedical Materials Research 47, 523–528.
Soares da Silva, M., Viveiros, R., Aguiar-Ricardo, A., Bonifacio, V., Casimiro, T., 2012. RSC Advances http://dx.doi.org/10.1039/c2ra20426f.
Sonesson, A.W., Blom, H., Hassler, K., Elofsson, U.M., Callisen, T.H., Widengren, J., Brismar, H., 2008. Journal of Colloid and Interface Science 317, 449–457.
Sunayama, H., Ooya, T., Takeuchi, T., 2010. Biosensors and bioelectronics 26, 458–462.
Tajima, N., Takai, M., Ishihara, K., 2011. Analytical Chemistry 83, 1969–1976.
Turro, N.J., Lei, X.G., Ananthapadmanabhan, K.P., Aronson, M., 1995. Langmuir, 2525–2533.
Ueda, T., Oshida, H., Kurita, K., Ishihara, K., Nakabayashi, N., 1992. Polymer Journal 24, 1259–1269.
Vasilescu, M., Angelescu, D., 1999. Langmuir 15, 2635–2643.
Wang, Y., Zhang, Z., Jain, V., Yi, J., Mueller, S., Sokolov, J., Liu, Z., Levon, K., Rigas, B., Rafailovich, M.H., 2010. Sensors and Actuators B 146, 381–387.
Watanabe, J., Ishihara, K., 2006. Biomacromolecules 7, 171–175.
Yaqub, S., Latif, U., Dickert, F.L., 2011. Sensors and Actuators B 160, 227–233.
Ye, L., Mosbach, K., 2008. Chemistry of Materials 20, 859–868.
Zhou, D., Guo, T., Yang, Y., Zhang, A., 2011. Sensors and Actuators B 153, 96–102.

Journal of Biomechanical Science and Engineering

Vol. 8, No. 3, 2013

Influence of Phospholipid and Protein Constituents on Tribological Properties of Artificial Hydrogel Cartilage Material*

Seido YARIMITSU**, Kazuhiro NAKASHIMA**,***, Yoshinori SAWAE**,*** and Teruo MURAKAMI**

** Research Center for Advanced Biomechanics, Kyushu University
744 Motooka, Nishi-ku, Fukuoka 819-0395, Japan
E-mail:yarimitsu.seido.681@m.kyushu-u.ac.jp

*** Department of Mechanical Engineering, Faculty of Engineering, Kyushu University
744 Motooka, Nishi-ku, Fukuoka 819-0395, Japan

Abstract

In this study, the influence of phospholipid and protein constituents on friction and wear behavior of artificial hydrogel cartilage was investigated. A sliding pair of an ellipsoidal specimen of poly (vinyl alcohol) (PVA) hydrogel and a flat specimen of PVA hydrogel was evaluated in simplified reciprocating friction test. Dipalmitoylphosphatidylcholine (DPPC) was selected as a phospholipid constituent and was dispersed in saline as liposome. Fluorescent-labeled albumin and γ-globulin were used as protein constituents in lubricants at concentration of 0.7 wt%. After reciprocating friction test, the boundary film formed on the surface of PVA hydrogel and the worn surface of PVA hydrogel were observed by using fluorescent microscope and confocal laser scanning microscope, respectively. When only albumin or γ-globulin was added to lubricant, adhesive wear pattern was frequently observed and large breaking-off of surface structure of PVA hydrogel occurred. Lubricants that contain both proteins and 0.01wt% DPPC showed reduction of friction and suppression of large breaking-off of surface structure of PVA hydrogel. Meanwhile, under coexistence of protein and 0.02wt% DPPC, friction increased compared to that for lubricants that contain 0.01wt% DPPC and the adhesive wear patterns became obvious. Therefore, both the concentration and the relative ratio of proteins to phospholipids are important factors to function adequately as excellent boundary lubricant for PVA hydrogel.

Key words: Artificial Hydrogel Cartilage, Phospholipid, Protein, Friction, Wear

1. Introduction

Total joint replacement has made significant contributions to better recovering of the articular joint function for patients of osteoarthritis and rheumatoid arthritis. Several materials such as biocompatible polymers, metals and bioceramics are applied as bearing materials of artificial joints. Ultra-high molecular weight polyethylene (UHMWPE) is commonly used as a bearing material for artificial joints. However, the loosening and the failure of artificial joint occur due to biological reaction to wear particles of UHMWPE[1,2]. Therefore, to extend the viability of joint prosthesis, the improvement of wear resistance of UHMWPE has been widely studied[3-5]. In metal-on-metal and ceramic-on-ceramic hip joints, the effective formation of fluid film was indicated[6,7]. However, metal ion release from metal component and fracture of ceramic component remained to be solved. As a

*Received 3 May, 2013 (No. 13-00051)
[DOI: 10.1299/jbse.8.257]

consequence, the improvement of lubrication mode in artificial joint by mimicking of the excellent lubrication mechanism of natural joint is also proposed.

Application of soft materials as artificial cartilage to bearing materials of artificial joints was proposed to improve the lubrication mode of artificial joints[8,9]. Many researches on the artificial cartilage have been conducted[10-12], and poly (vinyl alcohol) (PVA) hydrogel is one of the anticipated materials for artificial cartilage. Enhancement of fluid film formation by soft elastohydrodynamic lubrication (EHL) is expected by using PVA hydrogel as material for bearing surfaces, and it was reported that PVA hydrogel showed low friction at steady walking condition in knee joint simulator test[13]. However, considerable wear of PVA hydrogel occurs in severe condition like mixed or boundary lubrication due to poor wear resistance and mechanical strength[14,15]. To achieve the clinical application of PVA hydrogel as artificial cartilage, it is important to elucidate the wear mechanism of PVA hydrogel under the condition lubricated by body fluid. In joint cavity, synovial fluid is supplied mainly through synovial membrane and functions as lubricant for natural and artificial joint. Synovial fluid contains many biomolecules such as proteins, lipids and hyaluronic acid and it is indicated that those constituents influence on friction and wear behavior of artificial joint materials[16,17]. Therefore, it is important to elucidate the function of synovial fluid constituents as lubricant for PVA hydrogel to propose the improving method for wear reduction and material property modification considering the influences of synovial fluid constituents. In addition, the effect of intra-articular injection of some functional molecules such as hyaluronic acid[18], phospholipids[19] and proteins[20] on improvement of the lubrication of natural and artificial joints have been shown. For the application of some biomolecules to intra-articular injection, it is important to elucidate the mechanisms of lubrication by synovial fluid constituents.

In the previous study, it was found that the wear of PVA hydrogel depended on both the ratio and content of albumin and γ-globulin being mixed into lubricants[21]. It was indicated that the structure of protein boundary film on PVA hydrogel surface was the key essence for wear reduction [22]. In addition, it was indicated that the stability of protein boundary film changes with the concentration and the addition ratio of proteins in lubricants through in situ observation on forming protein boundary film[23]. When phospholipid and proteins coexist in lubricants, sheet-like matters were formed on rubbing surface especially in the lubricants that contain both phospholipid and albumin, and they contributed to reduction in friction of PVA hydrogel[24]. However, an important influence of phospholipid constituent on wear behavior of PVA hydrogel has not been cleared yet.

In this study, phospholipid and proteins were selected as additives to test lubricants. And then, influence of phospholipid and protein constituents on friction and wear behavior of PVA hydrogel was investigated.

2. Experimental methods

2.1 Reciprocating friction test

Details of reciprocating friction tester used in this study are shown in Fig. 1. A sliding pair of an ellipsoidal (major axis: 40mm diameter, minor axis: 25mm diameter) reciprocating upper specimen of PVA hydrogel as 2mm thickness and a flat stationary lower specimen of PVA hydrogel was tested. PVA hydrogel used in this study is shown in Fig.2. PVA hydrogel was prepared by freezing-thawing method, and number of freezing-thawing cycles was 5 times. Polymerization degree and saponificaiton degree of PVA (Kishida Chemical Co. Ltd.) was 2000 and 98.4~99.8 mol%, respectively. The elastic modulus of PVA hydrogel was 1.2 MPa and equivalent water content was 79%. The applied load was 2.94 N and average contact pressure was 0.093 MPa. Sliding speed of 20 mm/s was selected and the reciprocating stroke was 35 mm. Total sliding distance in this study was 1.5km.

Lubricant compositions used in this study are shown in Table 1. Normal saline solution (Otsuka Pharmaceutical Factory, Inc.) was used as solvent for lubricants. L-α dipalmitoyl phosphatidylcoline (DPPC) (Wako Pure Chemical Industries, Ltd.) was selected as a phospholipid constituent. DPPC is a main constituent of phospholipids in natural synovial fluid. DPPC was dispersed as liposomes in saline by ultra-sonication method. Bovine serum albumin (Wako Pure Chemical Industries, Ltd.) and human serum γ-globulin (Wako Pure Chemical Industries, Ltd., Japan) were used as protein constituents. The concentrations of each constituent were within the physiological range in natural synovial fluid[25,26]. Phospholipid concentration in synovial fluid changes with the condition of synovial joints and individual differences[26], and the concentration of DPPC in this study is within the range of healthy and postoperative synovial fluid. Albumin and γ-globulin were fluorescently labeled by rhodamine-B-isothiocyanate (Sigma Aldrich Co.) and fluorescein isothiocyanate isomer I (Sigma Aldrich Co.), respectively. Concentration of proteins in this study is within the physiological concentration but relatively low[27].

After friction test, protein boundary film formed on PVA hydrogel was observed by using fluorescent microscope (IX 71, Olympus Corporation). Then PVA hydrogel specimens were washed with solution of surface active agent to remove the adsorbed molecules and the worn surface of PVA hydrogel was observed by using confocal laser scanning microscope (VK-8500, Keyence Corporation).

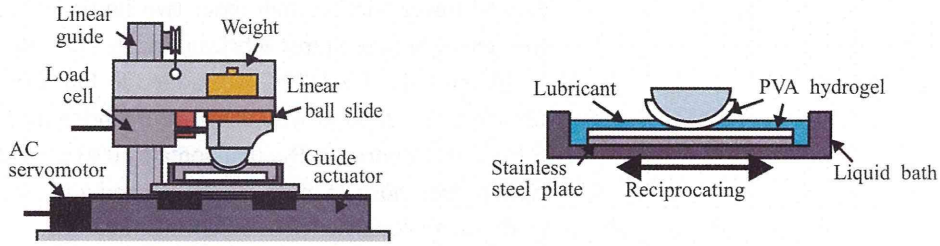

(a) Schematic view (b) Detailed view

Fig.1 Schematics of reciprocating friction tester

Fig. 2 PVA hydrogel prepared by freezing-thawing method

Table 1 Composition of lubricants

Lubricant	DPPC [wt%]	Albumin [wt%]	γ-globulin [wt%]
A	0	0	0
B		0.7	0
C		0	0.7
A_{P1}	0.01	0	0
B_{P1}		0.7	0
C_{P1}		0	0.7
A_{P2}	0.02	0	0
B_{P2}		0.7	0
C_{P2}		0	0.7

2.2 TEM observation of lubricant components

To reveal the influence of the lubricant composition on the morphology of the complexes of DPPC and proteins, lubricant components were observed by transmission electron microscope (TEM) before friction test. The lubricants shown in Table 1 were prepared and stored at room temperature for 6 hours. They were diluted a thousand fold by pure water to observe each component clearly and these were used as sample solutions. The copper TEM grid (Nisshin EM Corporation) was hydrophilized by using Plasma Ion Bombarder (PIB-10, Vacuum Device. Inc.) to prevent the aggregation of sample molecules on TEM grid. Then TEM grid was put on the 10μL droplet of diluted lubricant for 30s. Then, the residue of sample on copper TEM grid was absorbed by using filter paper. For negative staining of adsorbed molecules on TEM grid, samples were treated by 2.0 % solution of uranyl acetate for 30s. Finally, treated TEM grids were dried in air. The samples were observed by using transmission electron microscope (HT7700, Hitachi Hi-Technologies Corporation) operated at 100kV.

3 Results

3.1 Reciprocating Friction Test

Transients of friction coefficient during friction test in lubricants that contain no DPPC were shown in Fig.3 (a). When only single protein was added to lubricants, lubricant B showed lower friction than other two lubricants at initial state. However, there were little differences between three lubricants at steady state.

When 0.01wt% DPPC was added to lubricants, friction at initial state was reduced in lubricants A_{P1} and C_{P1} with comparing lubricants A and C that contained no DPPC as shown in Fig.3 (b). Lubricant B_{P1} that contains 0.01wt% DPPC and 0.7wt% albumin showed lower friction than those of other lubricants, and addition of 0.01wt% DPPC significantly reduced friction with coexistence of albumin and DPPC.

When only DPPC was added at a concentration of 0.02wt%, friction coefficient at initial state increased and the effect of friction reduction at steady state was slight as compared to that of 0.01wt%. In lubricants that contain proteins and 0.02wt DPPC, addition of DPPC with high concentration led the increase of friction (Fig.3 (d))

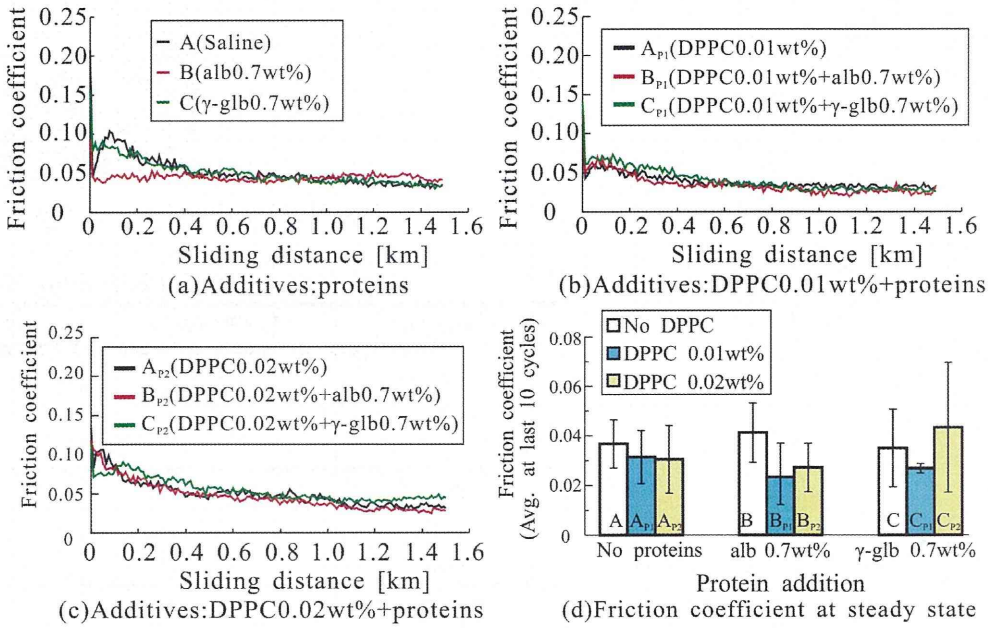

Fig.3 Friction coefficient during the reciprocating friction test and at steady state

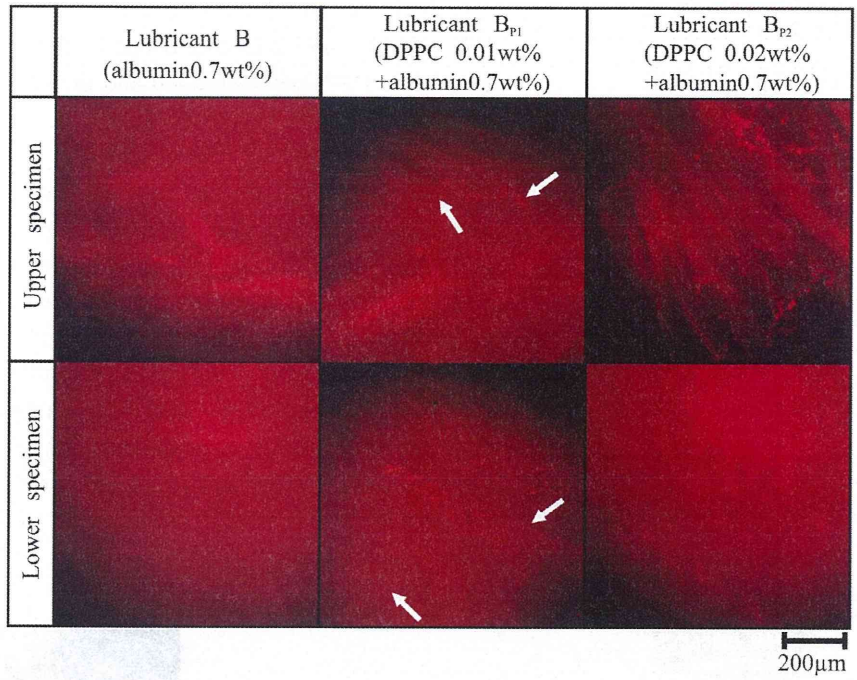

Fig.4 Fluorescent images of albumin film on PVA hydrogel

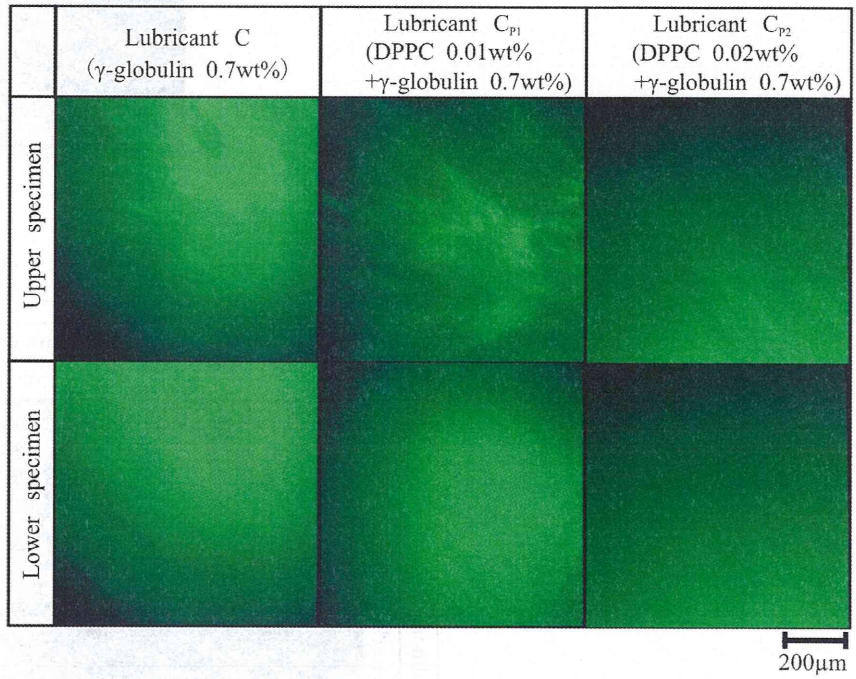

Fig.5 Fluorescent images of γ-globulin film on PVA hydrogel

The images of protein boundary film on PVA hydrogel by fluorescent observation were shown in Fig.4. Formation of smooth sheet-like adsorbed matters was observed in lubricant B_{P1} that contained 0.01wt% DPPC and albumin (Fig.4, arrows). However, degradation of forming sheet-like film was confirmed in lubricant B_{P2} that contained 0.02wt% DPPC. When lubricants contained γ-globulin as protein constituents, no sheet-like film was formed under coexistence of DPPC (Fig. 5).

Intact surface of PVA hydrogel and worn surfaces of PVA hydrogel as lower specimen were shown in Figs. 6 and 7, respectively. In normal saline, significant wear occurred with breaking off of the surface structure (Fig.7 (A)). In lubricant that contains albumin or

γ-globulin but no DPPC, severe wear occurred with loss of intact surface structure (Figs.7 (B), (C)). In lubricants that contain DPPC but no protein, severe abrasive wear occurred under low DPPC concentration and the reduction of wear was observed under high DPPC concentration (Fig.7 (A_{P2})). Wear reduction of PVA hydrogel was also confirmed in lubricant that contains protein and 0.01wt% DPPC (Figs. 3 (B_{P1}), (C_{P1})). However, both abrasive and adhesive wear patterns were observed in the lubricants that contains protein and 0.02wt% DPPC. These results indicated that DPPC contributes to reduction of friction and adhesivity and shifted the wear mode of PVA hydrogel from adhesive wear to abrasive wear. In addition, DPPC with high concentration and coexistence of DPPC with low concentration and protein reduce wear of PVA hydrogel. However, coexistence of DPPC with high concentration and protein has little effect in reducing wear of PVA hydrogel.

Worn surfaces of PVA hydrogel as upper specimen were shown in Fig.8. In lubricant A_{P1}, severe abrasive wear pattern with many scratches was confirmed. In contrast, significant wear occurred with breaking off of the surface structure in other lubricants. For all cases, there was no effect of lubricant additives on surface protection of PVA hydrogel as upper specimens.

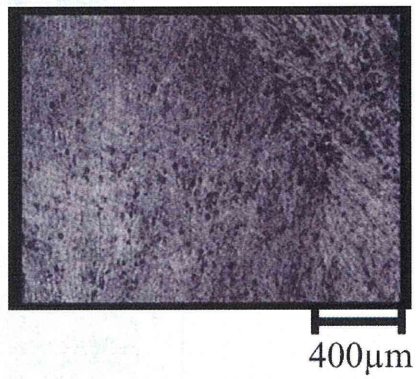

Fig.6 Intact surface of PVA hydrogel

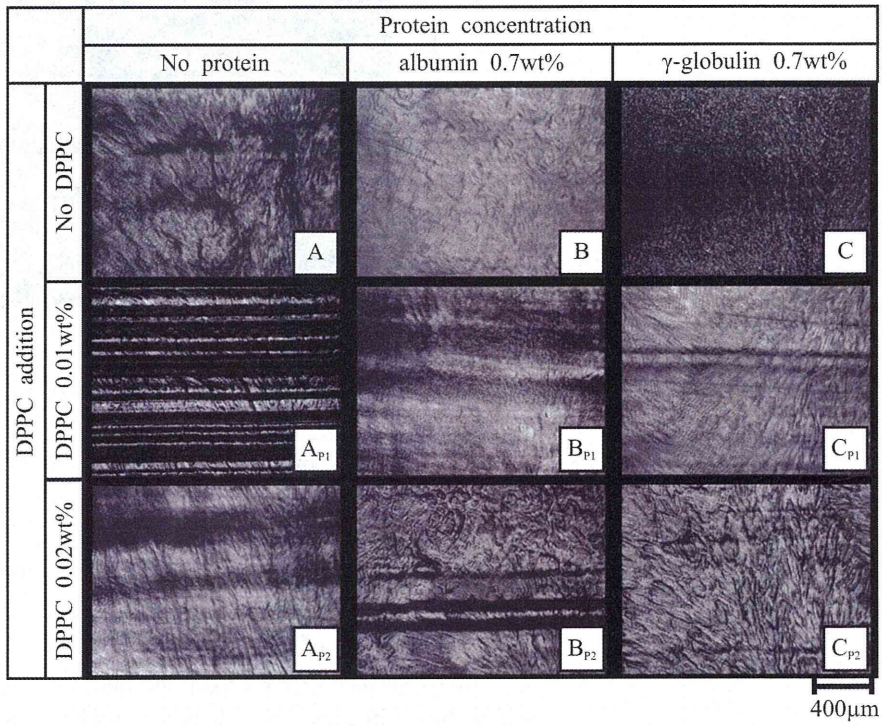

Fig.7 Worn surface of PVA hydrogel as lower specimens